Sensing slip of grasped wet, conformable objects

Natalie Burkhard[1], Ryan Steger[2], Mark Cutkosky[1]

***Abstract*— Grasping and manipulation of biological tissue are crucial processes during minimally invasive surgery (MIS). To enable atraumatic and reliable grasping, it would be useful to detect slip of the grasped object. Because tissue is moist, conformable, and delicate, and because the sensor must work in a surgical environment, this application requires a departure from conventional slip sensing methods. We present a technology and method based on hot-wire anemometry to detect slip while grasping wet, conformable materials and discuss how this approach may be extended to graspers used in robot-assisted surgery (RAS). We present our design and the results from characterization tests as well as experimental results that demonstrate its ability to detect planar direction of slip of wet, compliant objects.**

I. Introduction

A. Motivation and Application

Preventing slip of biological tissue during grasping is an important problem in surgery. Tissue grasping and manipulation enable standard tasks like dissecting, moving, stabilizing, and suturing tissue, but they require surgeons to balance two competing goals: maintaining grasp stability while avoiding damage due to excessive grip force [1]. In minimally invasive surgery (MIS) and robot-assisted surgery (RAS), this is made more difficult by the small size of the instruments' jaws, which makes it challenging to avoid applying high pressures [2]. Surgeons attempt to maintain their view and control tissue position by tailoring their selection of grasper type to the given task and modulating the grasper jaws to provide just enough force to prevent tissue slip, but not so much that damage occurs.

Applying excessive force to tissue can have serious consequences for the patient: tissue injury can lead to cell death, and torn tissue can be difficult to detect immediately. These can lead to sepsis and serious infections, particularly if tears occur in the small bowel. To avoid crushing tissue, surgeons may apply insufficient force to manipulate the tissue, causing it to slip from their grasp. This lengthens the procedure and reduces surgeons' confidence in their tools, both of which increase the opportunities for errors and complications. In a study of laparoscopic colectomy, Heijnsdijk et al. [3] reported a success rate of only 63% of grasping actions with 7% of failures attributed to tissue slip, of which about half resulted in trauma. Some surgeons experienced with RAS resort to alternative grasping methods to avoid causing trauma; e.g., using the instrument shaft rather than the jaws to manipulate delicate tissue.

[1]Dept. of Mech. Engineering, Stanford University, Stanford, CA 94305
ntb@stanford.edu, cutkosky@stanford.edu
[2]Intuitive Surgical, Inc., Sunnyvale, CA 94086
ryan.steger@intusurg.com

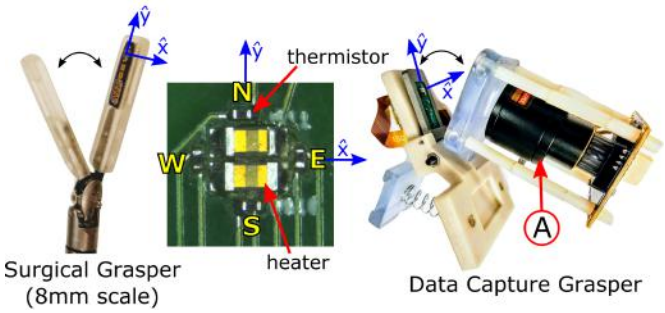

Fig. 1. ***Left***: Slip sensor mounted in 3D printed adapter on a modified Intuitive Surgical Long Tip Forceps for future studies. ***Center***: Prototype slip sensor used for data collection. Four thermistors are arrayed around 2 heating resistors and denoted N, S, E, and W; S-N direction corresponds to $+\hat{y}$ and W-E to $+\hat{x}$ as shown. ***Right***: 3D-printed grasper. Grasping region is enlarged to allow for video capture via camera Ⓐ as a ground truth for motion analysis.

Although some researchers have sought to use grip force feedback to address this problem, the maximum force with which one can atraumatically manipulate tissue and maintain grasp stability varies by tissue type [4], [5], jaw geometry [6], and other situational factors; realistically, implementation would be technically complex and require empirical tuning. Furthermore, [7] found that grasping control is more efficient when based on slip-related signals as opposed to signals related to exerted finger force. Thus, as in [1], we propose that a tissue slip sensor more directly addresses the fundamental problem of ensuring efficient grasping during MIS.

Slip detection is essential for grip force regulation, manipulation, and tactile exploration [8]; it is particularly important during MIS. Sensing slip of grasped *rigid* objects with Coulomb friction is a well-studied problem with many workable solutions [9]. *However, sensing slip of wet, deformable objects (such as biological tissue) poses many additional challenges because wet slip lacks the stick-slip vibrations that tend to signal incipient slip (slip that occurs in a narrow region of the contact surface and precedes macro slip) in dry scenarios* [8]–[10].

Sensing slip in MIS introduces additional requirements: solutions must be capable of sensing slip of wet, compliant objects and have the potential for integration into MIS or RAS end effectors, e.g. Intuitive Surgical's da Vinci EndoWrist® instruments. Integration into the end effector imposes significant packaging constraints. Slip is most easily sensed near the event of interest, so the sensor must fit into the grasper jaws or at least pass through the bore of a standard laparoscopic trocar. Furthermore, to facilitate surgeon acceptance, our technology must only minimally change the nature of the grasper jaws. Here we present a

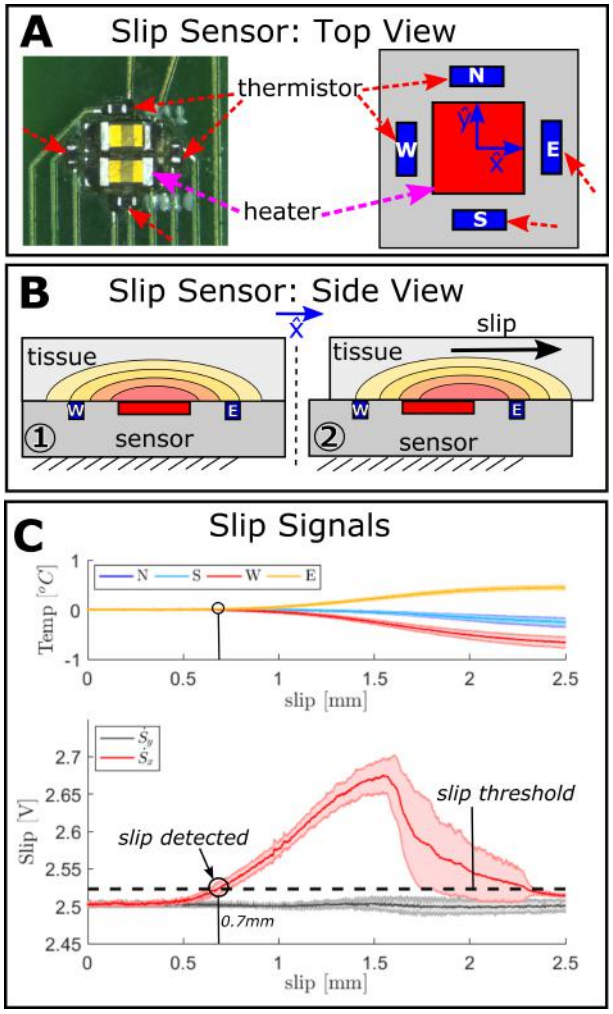

Fig. 2. **A**: Slip sensor top view with labeled N, S, E, and W thermistors. **B**: Cross-sectional view through E and W. Heater emits thermal energy conductively transferred to the thermistors (mainly through the grasped object) when stationary ①. When the object slips ②, E senses a temperature increase above baseline while W senses a decrease. N and S remain near baseline. **C**: Representative data for a slip from W to E; mean value across 10 trials and 1 standard deviation are plotted. Upper plot shows described temperature readings. Lower plot shows the output slip signal, $\dot{S}_x$; a nearly unchanged $\dot{S}_y$ is shown for comparison. The dashed black line denotes the slip threshold of 3 standard deviations above the mean baseline slip signal; here, slip is detected within 0.7 mm. Data is from turkey tissue[1].

proof-of-concept technology that has high applicability to RAS, can sensitively and specifically indicate the presence of slip and its direction, and is robust to mechanical noise or environmental impacts.

B. Related prior work

Dry, rigid-body slip is a relative displacement between two surfaces [8], [9]; see Francomano et al. [8] for a thorough review of slip sensors. Displacement-based slip sensors detect motion between two surfaces and may rely on mechanical parts joined to magnetic or optical transducers, but the interstitial spaces between moving parts are difficult to clean. More recent sensors compare CMOS sensor-acquired image sequences which are analyzed to obtain slip speed and direction. These present computational challenges for rapid motion analysis and packaging challenges for integration into the jaws of a surgical instrument.

Other sensors – including thick film PZT cantilevers, PVDF film transducers, accelerometers [11], and acoustic emissions detectors [12] – detect the stick-slip microvibrations that tend to signal incipient slip between contacting dry surfaces with Coulomb friction [10]. However, these vibrations are no longer present or are severely attenuated when the slipping object is wet and compliant. Brown et al. [13] added brass ridges to the jaw's contact surface and detected slip by monitoring pressure changes with PVDF, but their results stated that even with this mechanical amplification and alteration to the jaws, false positives were common.

Force transducers for slip sensing often sense changes in pressure distribution or surface deformations. These designs present miniaturization challenges and the likelihood of incurring false positives and negatives. The nature of conforming contact may cause changes in pressure distribution without slip occurring, but slip may also occur without accompanying force changes. Designs that seek to estimate the grip force required to balance the shear force or to detect the transition between static and dynamic friction are ill-suited to this application: the friction coefficient between the tissue and grasper jaw is difficult to estimate and changes with time, trauma, tissue type and other physiological factors. Stoll and Dupont [1] presented an approach that requires tangential grasp force measurement and differentiating relaxation and friction forces. However, this method may require modifications to the grasping surface to amplify friction forces and may be inaccurate if pressure concentrations are present.

Finally, a class of slip sensors senses temperature changes associated with mechanical slip [14], [15]. Based on hot-wire anemometry, these sensors use a thermal probe to maintain a heater at constant temperature, which requires nearly constant power. When slip occurs, a convective heat transfer term is introduced to the simple conduction problem, and the power required to maintain a constant temperature increases; the slip sensor monitors this change. Acknowledged drawbacks of this design are its inabilities to differentiate between making/breaking contact and slip, or to sense slip direction. The sensor presented here (fig. 1) is inspired by [14], [15]. However, our design relies on relating changes in spatial temperatures rather than changes in heating power, which can enable sensing directionality of motion (fig. 2).

II. Methods

A. Slip sensor design

As shown in figs. 1 and 2A, the sensor consists of four thermistors are arranged around a heating element and

[1]Raw "turkey bacon" (imitation bacon made of reconstituted turkey meat) was selected for data collection. Slices are consistent, homogeneous, and unlikely to tear unexpectedly. The thin slices provide uniform deformation throughout their thickness, crucial for DIC analysis. The slip sensor performed as well on pork loin, and chicken heart and gizzard, but thick tissue resulted in poor DIC (ground truth) planar deformation estimates.

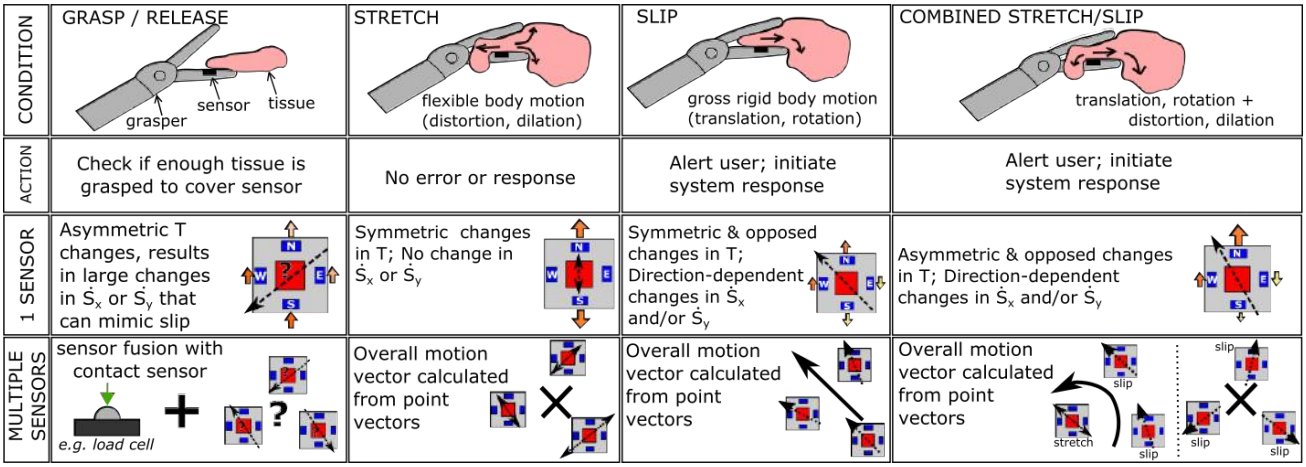

Fig. 3. Contact events likely to occur during RAS, the desired system action, and the conditions a single sensor and an array of multiple sensors will experience. Note that grasp/release may result in asymmetric changes as shown; perfectly even contact would result in common mode temperature and temperature derivative changes. The information one can obtain from a single sensor is limited to a motion vector. If three sensors are arrayed in the plane of the grasper jaw, one can estimate the tissue's planar deformation and extract the rigid body components of the motion (see explanation in text below). To effectively reject making or breaking contact with tissue (*column 1*), sensor fusion with a contact sensor is currently required.

embedded in a grasper jaw. The slip sensor has a surface area of 3.5x3.5 mm^2; the overall PCB is 7x26 mm^2.

The thermistors (NTCG063JF103FTB, TDK Corp.) are named after the cardinal directions (N,S,E,W); in the plane of the jaw, $\hat{x}$ corresponds to W-E, and $\hat{y}$ corresponds to S-N. This thermistor was selected for its low cost, fast response, and compact package. The thermistors' resistances are converted to voltages using transimpedance circuits. Temperature is calculated from resistance using the Steinhart-Hart equation:

$$\frac{1}{T} = A + B[ln(R)] + C[ln(R)]^3 \tag{1}$$

where $A = -2.2 \times 10^{-3}$, $B = 7.9 \times 10^{-4}$, and $C = -2.2 \times 10^{-6}$ (fit against a thermocouple in a water bath and checked against manufacturer-provided calibration data). Opposing pairs of thermistors (N-S, W-E) are fed into instrumentation amplifiers to amplify their differences: $S_x = T_E - T_W$, $S_y = T_N - T_S$. These are differentiated to produce slip signals $\dot{S}_x$ and $\dot{S}_y$, which are amplified and centered about 2.5 V (see Section II-B for relation to slip).

The heater (a pair of 49.9Ω Vishay Thin Film resistors in series, PCAN0603E49R9BST5) is resistively heated at 110 mW. This heating power was selected after preliminary tests to determine the maximum heating power that does not result in exceeding 45^oC limit for direct tissue contact safety [16]. 110 mW results in ~43^oC over 10 minutes.

The slip sensor substrate was designed to minimize internal conduction (minimal copper near the thermistors and heater) because, ideally, the thermistors would sense temperature changes at the grasping contact interface and not through the substrate. To create a smooth contact interface, the resistors and thermistors are coated up to the level of the tallest component (0.5 mm) in Loctite 435 ™(Henkel Corporation), selected for its low thermal conductivity.

B. Sensing strategy

When tissue comes in contact with the jaw, heat is conducted from the heating element into the tissue, forming a thermal gradient $T(x, y, t)$ in it. As in [14], [15], we approximate this heat transfer problem as:

$$\frac{\partial T}{\partial t} = \kappa \nabla^2 T - v \cdot \nabla T + \dot{q}(x, y) \tag{2}$$

where $\dot{q}(x, y)$ $[\frac{W}{m^3}]$ is the heat source, κ $[m^2/s]$ is the thermal diffusivity of the grasped tissue, and $v \cdot \nabla T$ is the convection term that models the slip of the tissue against the sensor; this term is zero if no motion is present.

If tissue moves over a thermistor, there will be a signal in proportion to the change in temperature. In general, local tissue movement can arise from any combination of *motion* (translation and rotation) and *deformation* (dilation, extension, and shear) [17]. For slip sensing, we are interested in translation. With a single sensor we cannot entirely separate the effects of motion and deformation because distinguishing them requires multiple points of measurement and a sense of scale: a microscale slip may be part of a macroscale slip *or* stretch, and motion may have both rigid and deformation components (fig. 3). However, we can construct signals, $\dot{S}_x$ and $\dot{S}_y$, that respond primarily to translation in the $\hat{x}$ and $\hat{y}$ directions, respectively.

We note that for a translation, and assuming an approximately symmetric heating zone, the thermistor in the leading direction should experience an increase in temperature while the thermistor in the trailing direction should experience a temperature decrease. Therefore, we define slip signals as $\dot{S}_x = \frac{\partial}{\partial t}(T_E - T_W)$ in the $\hat{x}$ and $\dot{S}_y = \frac{\partial}{\partial t}(T_N - T_S)$ in the $\hat{y}$. Time derivatives are used to avoid reliance on magnitude. Note that dilation (as may occur when increasing the grasp force on a piece of tissue so that it expands radially) will produce no signal because the thermistors' temperatures will decrease together. A pure rotation will also produce no

signal, due to symmetry.

The signals $\dot{S}_x$ and $\dot{S}_y$ are, of course, imperfectly correlated with slip. The temperatures measured at each thermistor also depend on the history of heating and tissue movement and on the overall conduction and convection at the boundaries. This sensing strategy is also not robust to uneven contact or release of tissue, which causes unpredictable changes in the four sensed temperatures and can mimic slip. However, for realistic grasping scenarios, $\dot{S}_x$ and $\dot{S}_y$ provide a useful single-point indicator of slip occurrence and direction. Using an array of such sensors, a topic for future work, would enable estimation of the tissue's planar motion and deformation over the grasper jaw. Our goal here is to produce a directional signal in response to 1 mm of slip (approximately half a standard jaw width).

This design is well-suited to sensing slip of biological tissue: by collecting redundant absolute measures of temperature, we can monitor a critical parameter tied to tissue damage. Furthermore, by collecting multiple measurements on a single input, varying moisture content or tissue thickness are common mode events that are rejected.

III. Experiments

Figure 4 illustrates the bench-top experimental setup made to imitate a MIS grasper. A DAQ (Sensoray826, Sensoray) reads the analog output from 4 thermistors (N,S,W,E), the thermistor pair differences (S_y, S_x) and their derivatives ($\dot{S}_y$, $\dot{S}_x$), and a single-axis button-type load cell (FSS015WNGX, Honeywell) into a custom C++ program. The heating circuit maintains constant power (110 mW); it is left on to simulate real use. The load cell was centered below the slip sensor to obtain grip force.

Video was recorded at 60 fps with 1280x720 pixels resolution using an ELP-USBFHD01M-L21 camera (Ailipu Technology Co., Ltd) calibrated with the MATLAB Camera Calibration toolbox. Videos were used to perform digital image correlation (DIC) to estimate displacements at the contact interface and ensure slip (rather than stretch) occurred during testing. DIC is a ubiquitous non-contact technique for measuring material displacement and deformation based on the comparison of two images acquired at different states, before and after motion. Here, DIC was performed in MATLAB using Ncorr, an open source 2D-DIC MATLAB software [18]. To aid DIC analysis, grasped objects were stained with randomly placed dots of black food coloring. The grasped object was displaced using a custom system based on a monocarrier (MCM03015P02K, NSK Global), a linear slide (6709K301 and 6709k120, McMaster-Carr), and a SmartMotor (Moog Animatics). Accuracy of Ncorr and the SmartMotor system were validated using a laser displacement sensor (LK-H082, Keyence); displacements agreed within 0.5% of desired motion.

Tests were conducted to test the effectiveness of our sensor. The sensor was operated as described; four thermistors were sampled and the differences between opposed pairs were differentiated to obtain the slip signals as described in the previous section. The slip sensor was mounted in one

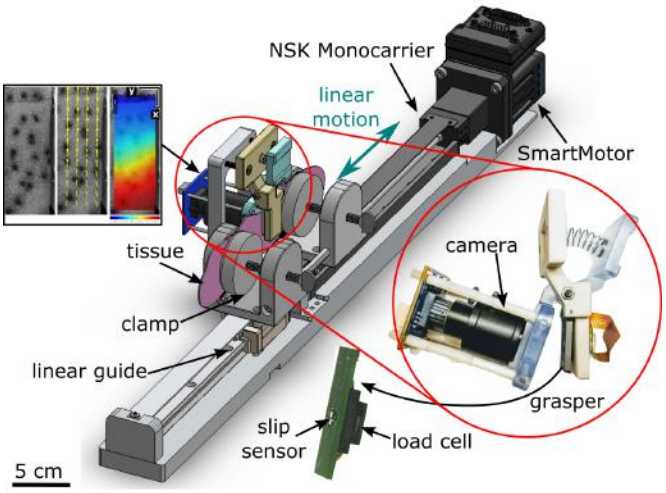

Fig. 4. Experiment setup for commanding slip trajectories and measuring slip. **Right inset** shows the grasper; the jaw-mounted camera obtains video of the planar tissue deformation. On the underside of the slip sensor board, a load cell collects grasp force. **Left inset** depicts DIC analysis on speckled foam. Left image is the 'reference' image. Middle image is taken 0.5 s later; the vector field of Lagrangian displacements w.r.t. the reference image is overlaid. Right image shows a Ncorr colormap output of the x displacements; color gradient shows increasing displacement from bottom to top, implying stretch.

jaw of a rigidly-mounted 3d-printed grasper. A force sensor under the slip sensor allows the grip force to be precisely set prior to each trial. The other grasper jaw contains an optically clear window to allow video capture of the grasped tissue for motion analysis. Thin samples of tissue were used to obtain more accurate planar deformation estimates. Tissue is held in two clamps mounted on a passive linear guide carriage and a linearly actuated carriage. The passive carriage is linked rigidly to the other carriage to mimic tissue slip through the grasper. Rigid-body motion of the tissue is enforced by imposing slip trajectories with the SmartMotor and checking homogeneity of motion using DIC analysis.

IV. Results

The results from tests comparing two speeds of slip in the $+\hat{x}$ direction are shown in fig. 5. Grip force was set at a relatively low value (0.5 N) to allow nearly rigid-body motion with minimal stretch (confirmed with DIC). Fluctuations in grip force associated with slip were present but with a poor signal-to-noise ratio. As expected, $\dot{S}_x$ changes repeatably in response to slip while $\dot{S}_y$ remains approximately unchanged.

Figure 6 presents results from tests where the acceleration (velocity ramp rate of the controlled stage) of slip was varied. The rate of change of slip signal with slip distance is the same regardless of the acceleration. We hypothesize that for faster slip, the tissue moves faster than it is locally heated, so the signal continues to grow. For slower slip, convection is less, so the slip signal reaches a lower maximum. We anticipate that this result will be consistent with higher speeds up until some maximum where the tissue is moving so fast that the sensors cannot obtain a measurement.

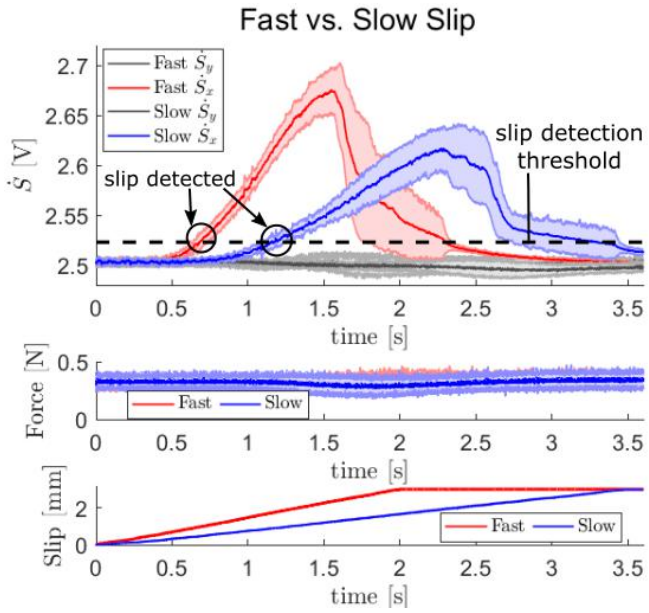

Fig. 5. Results from 10 trials each of fast (0.61 mm/s^2) and slow (0.12 mm/s^2) slip of room temperature tissue slipping through the grasper in $+\hat{x}$ for 3 mm (*row 3*); mean and standard deviations are shown. Grip force was set at 0.5 N for all trials (*row 2*). Row 1 shows the slip signals; there is clearly a $\dot{S}_x$ response but no $\dot{S}_y$ response. The dashed black line denotes a significant deviation ($\mu + 3 * \sigma$; $\mu = 2.504, \sigma = 6.4 * 10^{-3}$) above baseline slip signal levels, or the level at which we can identify slip. Minimum detectable slip levels ranged from 0.7-0.9 mm.

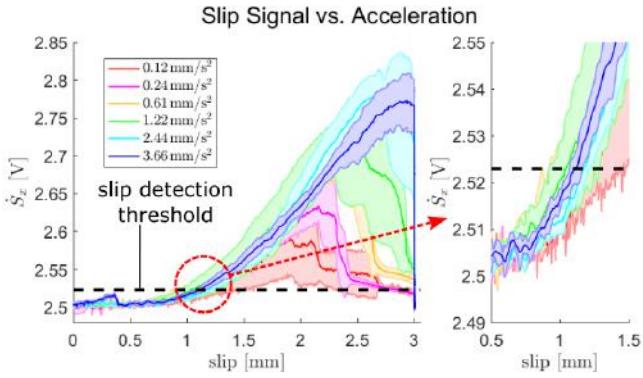

Fig. 6. $\dot{S}_x$ vs. slip displacement for different slip accelerations; 5 trials were conducted for each acceleration; mean and standard deviations are shown. As shown in the inset, the rate of change of slip signal with slip distance is independent of the acceleration. For faster slip, the tissue moves faster than it is locally heated, so the signal continues to grow. For slower slip, convection is less, so the slip signal reaches a lower maximum. As in fig. 5, the dashed black line denotes ($\mu + 3\sigma$) above baseline slip signal. Minimum detectable slip ranges from 0.87-1.4 mm.

V. DISCUSSION

During slip, the difference between opposed pairs of thermistors increases at a rate independent of slip speed or acceleration. Faster slips are accompanied by larger maximum slip signals because the tissue is moving faster than heat can be conducted through it. Grip force fluctuations do occur during slip, but the variations have a poor signal-to-noise ratio and are visually poor indicators of slip.

There are some error sources on the hardware side. Our signals rely on resistance measurements, so any asymmetry in the signal conditioning circuits (performance variations, manual potentiometers, component value tolerances) and amplifier nonidealities contribute to error. Furthermore, although the nichrome heating resistors were selected for their low temperature dependence, a value of zero is unachievable so the heating power does vary with temperature.

The tissue we tested was near room temperature (~$24 - 29^oC$) which is much cooler than the heating element (~42^oC). Tissue *in vivo* is likely much warmer, nearer to 37^oC. Cooler objects have steeper thermal gradients and therefore sharper changes in slip signals associated with slip; therefore, we can expect some reduced sensitivity *in vivo*.

The grasped object's properties affect sensor performance. Slip signals are larger when the grasped object has lower specific heat capacity and/or less mass between the grasper jaws: objects with these characteristics require less heat to locally change their temperature. This means that the region of the grasped object in contact with the slip sensor can more quickly establish a steep thermal gradient, which will enable a clearer response from the sensor more quickly.

VI. CONCLUSIONS AND FUTURE WORK

A. Conclusions

This paper presents a slip sensor whose working principle takes inspiration from hot-wire anemometry. The presented sensor has the additional ability to inform directionality of slip in addition to detecting it within 1 mm. A heater keeps the sensor and its local environment above the environmental temperature. When the environment is stationary, the temperature at all four thermistors changes approximately equally. When slip occurs, thermistors on opposite sides of the heater experience different temperature changes. Taking the derivatives of these temperature differences amplifies the sensitivity to slip. The temperature at each thermistor is a function of the speed of slip, the contact conditions and the thermal properties of the grasped object. However, the computed derivative slip signals are relatively independent of these variables. These results compare favorably with those in previous work (e.g. [15]).

B. Future Work

Our goal is to implement thermal slip sensing within the profile of the grasper jaws of a RAS instrument (see fig. 7). Our next efforts will focus on miniaturization, safety, and wiring. Miniaturization of the circuitry to contain all electronics in the jaw would facilitate sensor performance by increasing responsiveness, reducing thermal mass, and making uniform contact easier to achieve. Furthermore, as noted in [19], thermal phenomena are relatively slow, e.g. as compared to electromechanical ones. However, because the time constant is proportional to L^2, we can expect the response time to diminish as the linear dimension of the sensor is reduced, a result presented in [15].

Jaws vary widely in grasping surface dimensions (lengths range from 5-30 mm, widths from 3-8 mm), and many have fenestrations (holes) in the main grasping region, making

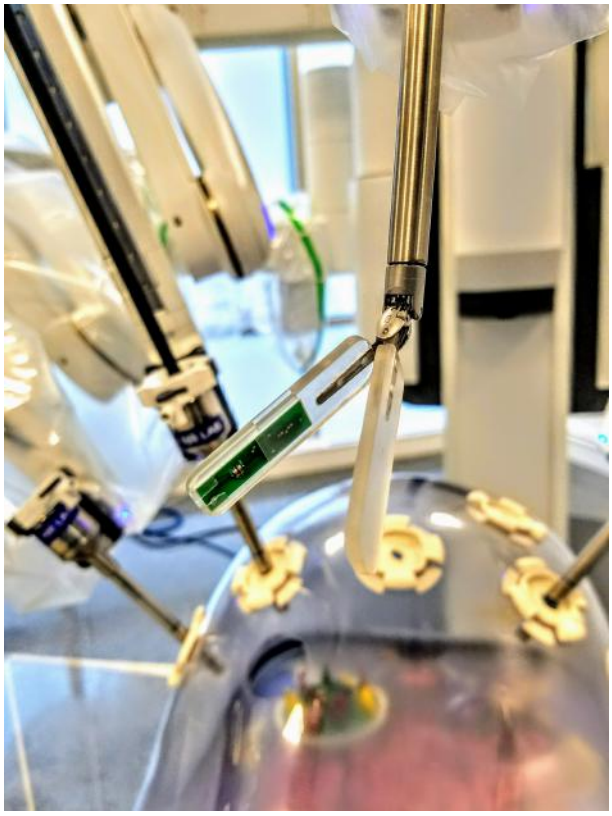

Fig. 7. Prototype slip sensor mounted on modified Intuitive Surgical Long Tip Forceps with 3D printed adapter.

packaging a difficult challenge. We are currently exploring SMT versions of this sensor as well as other more compact technologies.

While the heating element is currently powered open-loop; implementing closed-loop control would be straightforward and would allow us to maintain the highest permissible temperature gradient in warm tissue, thereby enhancing the device's safety and sensitivity.

By creating an array of our sensors, we can provide 2D planar deformation information across the sensing surface. Increasing the number of temperature sensors arrayed around each heating element will allow us to improve the accuracy of the slip direction vector at each sensing point. Wiring is a concern as well; the number of conductors that must be routed around or through the instrument wrist should be minimized. Once optimized, additional ex-vivo tissue grasping data will be collected with the sensor to explore performance on a variety of tissue types and under environmental conditions that better approximate surgery.

Finally, integration into a RAS system poses many challenges not yet addressed. Beyond robustly distinguishing slip from contact, there is the potential to provide feedback for tissue manipulation. In other work, [20] noted that tactile feedback proved more useful than visual feedback in displaying tissue slippage; however, transduction technologies are worth exploration. Furthermore, surgeons are not always grasping or trying to avoid slip. Avoiding presenting unwanted information is crucial to user acceptance. The presented work is a bench-top model and will require significant advances to prepare for clinical use and evaluation.

ACKNOWLEDGMENT

This work was supported by Intuitive Surgical, Inc., is a collaboration with the Biomimetics and Dexterous Manipulation Laboratory at Stanford University, and was performed at Intuitive Surgical's Advanced Product Development research laboratory in Sunnyvale, CA.

REFERENCES

[1] J. Stoll and P. Dupont, "Force Control for Grasping Soft Tissue," *Control*, no. May, pp. 4309–4311, 2006.

[2] J. A. Cartmill, A. J. Shakeshaft, W. R. Walsht, and C. J. Martin, "High pressures are generated at the tip of laparoscopic graspers," *Aust. N. Z. J. Surg.*, vol. 69, no. 2, pp. 127–130, 1999.

[3] E. A. M. Heijnsdijk, J. Dankelman, and D. J. Gouma, "Effectiveness of grasping and duration of clamping using laparoscopic graspers," *Surg. Endosc. Other Interv. Tech.*, vol. 16, no. 9, pp. 1329–1331, 2002.

[4] S. De, J. Rosen, A. Dagan, P. Swanson, M. Sinanan, and B. Hannaford, "Assessment of tissue damage due to mechanical stresses," 2006, pp. 823–828.

[5] S. De, "The Grasper-Tissue Interface in Minimally Invasive Surgery: Stress and Acute Indicators of Injury," Doctor of Philosophy, University of Washington, 2008.

[6] E. Heijnsdijk, "Tissue manipulation in laparoscopic surgery," Doctor of Philosophy, Delft University of Technology, 2004.

[7] T. D'Alessio and R. Steindler, "Slip sensors for the control of the grasp in functional neuromuscular stimulation," *Med. Eng. Phys.*, vol. 17, no. 6, pp. 466–470, 1995.

[8] M. Francomano, D. Accoto, and E. Guglielmelli, "Artificial Sense of Slip - A Review," *IEEE Sens. J.*, vol. 13, no. 7, pp. 2489–2498, 2013.

[9] M. R. Cutkosky and J. Ulmen, "Dynamic Tactile Sensing," in *Hum. Hand as an Inspir. Robot Hand Dev.*, 1st ed., ser. Springer Tracts in Advanced Robotics, R. Balasubramanian and V. J. Santos, Eds. Springer International Publishing, 2014, vol. 95, ch. 18, pp. 389–403.

[10] R. S. Johansson and J. R. Flanagan, "Coding and use of tactile signals from the fingertips in object manipulation tasks." *Nat. Rev. Neurosci.*, vol. 10, no. 5, pp. 345–59, May 2009.

[11] R. D. Howe and M. R. Cutkosky, "Sensing skin acceleration for slip and texture perception," in *IEEE Int. Conf. Robot. Autom. Proc.*, 1989, pp. 145–150.

[12] X. Wu, N. Burkhard, B. Heyneman, R. Valen, and M. Cutkosky, "Contact Event Detection for Robotic Oil Drilling," in *IEEE Int. Conf. Robot. Autom.* IEEE, 2014.

[13] A. Brown, S. Brown, Z. Wang, D. Maclean, and A. Cuschieri, "Development Of An Autonomous Smart Graspers To Prevent Tissue Slip During Laparoscopic Surgery," in *Soc. Am. Gastrointest. Endosc. Surg.*, 2013.

[14] D. Accoto, F. Damiani, R. Sahai, D. Campolo, E. Guglielmelli, and P. Dario, "A thermal slip sensor for biorobotic applications," in *Robotics and Automation, IEEE International Conference on*. IEEE, 2007, pp. 1523–1528.

[15] D. Accoto, R. Sahai, F. Damiani, D. Campolo, E. Guglielmelli, and P. Dario, "A slip sensor for biorobotic applications using a hot wire anemometry approach," *Sensors Actuators, A Phys.*, vol. 187, pp. 201–208, 2012.

[16] International Electrotechnical Commission, "IEC 60601-2-2: 2009: medical electrical equipment–Part 2-2: particular requirements for the basic safety and essential performance of high frequency surgical equipment and high frequency surgical accessories." Geneva, 2009.

[17] H.-C. Wu, *Continuum mechanics and plasticity*. CRC Press, 2004.

[18] J. Blaber, B. Adair, and A. Antoniou, "Ncorr: Open-Source 2D Digital Image Correlation Matlab Software," *Exp. Mech.*, vol. 55, no. 6, pp. 1105–1122, 2015.

[19] P. Dario, B. Hannaford, and A. Menciassi, "Smart Surgical Tools and Augmenting Devices," *IEEE Trans. Robot. Autom.*, vol. 19, no. 5, pp. 782–792, 2003.

[20] J. D. Westwood, "Tactile feedback exceeds visual feedback to display tissue slippage in a laparoscopic grasper," *Med. Meets Virtual Real. 17 NextMed Des. For/the Well Being*, vol. 142, p. 420, 2009.